RSC Advances

PAPER

View Article Online
View Journal | View Issue

Cite this: *RSC Adv.*, 2025, **15**, 27623

Triterpene saponins from the halophyte *Anabasis setifera* exhibit anti-SARS-CoV-2 properties

Ahmed Othman, *[a] Omnia Kutkat, [b] Samar S. Mabrouk [c] and Yhiya Amen *[d]

Received 1st May 2025
Accepted 29th July 2025

DOI: 10.1039/d5ra03089g

rsc.li/rsc-advances

Halophytes are well-known as a rich source of health-promoting phytochemicals. This study aimed to elucidate the chemical constituents and antiviral potential of the halophyte *Anabasis setifera* Moq., growing in the desert areas of Egypt. Six triterpenoid oleanane saponins (**1–6**) were purified using several chromatographic procedures and identified *via* HRMS and NMR spectroscopic analyses, with solysaponin **B–D** being reported for the first time. Additionally, three known triterpene saponins (**4–6**) were identified as spinacoside C (**4**), betavulgaroside IV (**5**), and (3β)-3-(β-D-glucuronopyranosyloxy)olean-12-en-23,28-dioic acid (**6**). The isolated triterpene saponins were able to inhibit the severe acute respiratory syndrome corona virus 2 (SARS-CoV-2). Our study provides valuable insights into the promising antiviral activity of saponins **1**, **2** and **4** with IC_{50} values ranged between 2.339 and 6.837 μg mL^{-1}.

Introduction

The global pandemic caused by the severe acute respiratory syndrome coronavirus 2 (SARS-CoV-2), which emerged in 2019, has resulted in millions of infections and deaths worldwide. This pandemic continues to be a major public health concern.[1,2] Although vaccination has reduced the infection rate, new virus strains have emerged, underscoring the need for potent antiviral drugs. Currently, tocilizumab, remdesivir, and baricitinib were approved as drugs for the treatment of SARS-CoV-2.[1] Notably, plant-based natural compounds represent a promising alternative for developing antiviral drugs, owing to their bioavailability, cost-effectiveness, and fewer side effects. Among these, saponins and other natural-derived products emerged as valuable sources for drug discovery, due to their structurally diverse scaffolds and high safety profile. Within natural products, halophytes are known to produce a wide variety of secondary metabolites, including saponins, alkaloids, lignans, and flavonoids.[3,4] Saponins are a diverse group of chemical constituents found in plants, particularly halophytes, with several biological activities.[5–7] These compounds are involved in the chemical defense of halophytic plants, enabling them to survive under harsh environments. The aglycone moieties of saponins in halophytes belong to the oleanane class with $\Delta^{12(13)}$ double bond and an oxygen atom at C-3. In addition to their role in plant defense, saponins serve as an important source of drug molecules due to their pharmacological properties.[8]

The Amaranthaceae family comprises about 175 genera and 2000 plant species that have diverse chemical scaffolds, nutritional and bioactive properties.[7,9] Plants within Amaranthaceae have an economic value and are used as herbal remedies for therapeutic purposes in various parts of the world.[7] Moreover, the phytochemical studies performed on Amaranthaceae plants revealed their content of saponins, essential oils, phenolics, flavonoids, and sesquiterpenoids.[3,7,9,10] It is worth mentioning that saponins have been reported from several Amaranthaceae plants.[7] Recent studies demonstrated that plants within Amaranthaceae exhibited antiviral, antidiabetic, antitumor, anti-inflammatory, anti-osteoporosis, larvicidal, and antihypertensive activity.[9,11]

The halophyte *Anabasis setifera* Moq. (Amaranthaceae) is widely distributed in Egyptian deserts and exhibits remarkable adaptability in harsh environments.[12] The chemical investigation of this plant species is still barely limited. Thus, the present study reports on the isolation and structure elucidation of new triterpene oleanane saponins from the methanol extract of the aerial parts of *A. setifera*. In the current study, six triterpene oleanane saponins were characterized in the plant *A. setifera*, and they were identified as solysaponin **B–D** (**1–3**), spinacoside C (**4**), betavulgaroside IV (**5**), and (3β)-3-(β-D-glucuronopyranosyloxy)olean-12-en-23,28-dioic acid (**6**). Besides, the anti-SARS-Cov-2 activity of triterpene saponins from *A. setifera* was evaluated.

Experimental

General experimental procedures

The NMR analysis was performed on a DRX-600 spectrometer (Bruker Daltonics, USA). The high-resolution mass

[a]Department of Pharmacognosy and Medicinal Plants, Faculty of Pharmacy (Boys), Al-Azhar University, Cairo 11884, Egypt. E-mail: ah.othman@azhar.edu.eg
[b]Centre of Scientific Excellence for Influenza Viruses, Water Pollution Research Department, Environment Research and Climate Change Institute, National Research Centre, Giza 12622, Egypt. E-mail: omnia.abdelaziz@human-link.org
[c]Department of Microbiology, Faculty of Pharmacy, Ahram Canadian University (ACU), 6th October City, Giza 12566, Egypt. E-mail: samar.mabrouk@acu.edu.eg
[d]Department of Pharmacognosy, Faculty of Pharmacy, Mansoura University, Mansoura 35516, Egypt. E-mail: yhiaamen@mans.edu.eg

spectrometry data of compounds was recorded on a quadrupole time-of-flight mass spectrometer (Agilent QTOF-LC-MS, Agilent Technologies, USA). Partitioning of fractions was carried out with a Diaion HP-20 purchased from Mitsubishi Chemical Corporation, Japan. Further, Medium Pressure Liquid Chromatography (MPLC Pure C-850 Flash prep®, Buchi, Switzerland) equipped with UV and ELSD detection and connected to a reversed-phase flash column (Flash pure C18, 40 μm; 40 g) was used for partitioning. A recycling preparative HPLC was performed on JAI liquid chromatography system (Labo ACE LC-5060 Plus II; Analytical Industry Co., Ltd, Japan) with UV adjusted to 205, 210, 230, 254 nm and refractive index detection. The final purification was performed on a preparative HPLC column (Inertsil ODS-3, 5 μm, 20 × 250 mm), obtained from GL Sciences Inc., Japan. TLC plates (Merck 60 F_{254}) were used for investigation of fractions and/or compounds. The TLC chromatograms were visualized by spraying with 10% H_2SO_4 solution and heating at 105 °C.

Plant material

The aerial parts of *Anabasis setifera* Moq. (Amaranthaceae) were collected from the desert areas of Wadi-Degla valley (30 km southeast Maadi City), Cairo, Egypt in September, 2019. The plant parts were identified by Prof. Ibrahim A. El-Garf, Department of Botany, Faculty of Science, Cairo University, Egypt. A voucher specimen (code no. AN-2019) of the dried sample has been kept in the herbarium of Pharmacognosy and Medicinal Plants Department, Faculty of Pharmacy, Al-Azhar University, Egypt.

Extraction and isolation

The air-dried aerial parts of *Anabasis setifera* (1.5 kg) were powdered and subjected to maceration three times with MeOH at room temperature to give a 260 g methanolic extract. The crude extract was suspended in H_2O and subjected to liquid–liquid extraction with *n*-hexane, CH_2Cl_2, and EtOAc to obtain *n*-hexane-soluble fraction (19.8 g), CH_2Cl_2-soluble fraction (14.1 g), EtOAc-soluble fraction (8.9 g), and aqueous fraction (212.0 g). The aqueous fraction (212.0 g) was mixed with Celite and partitioned over a Diaion HP-20 column and eluted with H_2O only to give two main fractions; H_2O-eluate 1 (108.0 g) and H_2O-eluate 2 (41.0 g); then, a gradient elution of H_2O–MeOH was applied to get ten fractions (Fr.1 to Fr.10).

Following TLC investigation, the fraction Fr.1 (2.25 g) was partitioned over reversed-phase C_{18} flash column (40 g)

Table 1 NMR data of the aglycone part of solysaponins B–D

	1		2		3	
Position	^{1}H	^{13}C	^{1}H	^{13}C	^{1}H	^{13}C
1	0.98, 1.58 m	38.3	0.96, 1.42 m	39.1	0.96, 1.42 m	38.1
2	1.60 m 1.85 m	26.3	1.88 (dd, J = 13.7, 4.0 Hz) 2.26 (dd, J = 13.7, 4.3 Hz)	26.7	1.88 m	26.0
3	3.97 m	86.4	4.68 (dd, J = 12.0, 4.5 Hz)	85.7	4.70 (dd, J = 12.1, 4.5 Hz)	85.0
4	—	39.5	—	40.7	—	39.8
5	1.51 m	52.8	1.89 m	52.6	1.86 m	51.8
6	1.12 m 1.49 m	21.7	1.43, 0.97 m	39.1	1.81 m	23.5
7	1.28 m 1.35 m	32.3	1.30, 1.03 m	34.4	1.21, 1.55 m	32.6
8	—	42.4	—	42.6	—	41.8
9	1.61 m	47.5	1.70 m	48.7	1.72 m	47.6
10	—	37.3		37.1	—	36.3
11	1.95, 1.95 m	26.3	1.90, 1.90 m	24.2	1.96, 1.96 m	23.7
12	5.25 brs	123.9	5.38 (t, J = 3.6 Hz)	123.2	5.43 (t, J = 3.8 Hz)	122.5
13	—	144.1	—	144.6	—	143.9
14	—	42.8	—	42.6	—	41.7
15	1.03, 1.42 m	28.8	1.29, 1.19 m	26.7	1.10 m	27.9
16	1.92 m	24.4	2.25, 1.88 m	28.7	1.87, 2.6 m	30.1
17	—	48.2	—	47.4	—	47.8
18	2.66 (dd, J = 13.5, 5.2 Hz)	48.5	3.15 (dd, J = 13.9, 4.9 Hz)	46.6	3.18 (dd, J = 13.5, 5.2 Hz)	46.8
19	2.48 (t, J = 13.6 Hz) 1.77 (d, J = 14.4 Hz)	42.5	1.70, 1.19 m	42.2	2.17, 2.51 m	41.8
20	—	149.2	—	31.3	—	148.8
21	1.85, 2.04 m	30.8	1.19, 1.43 m	33.0	1.86, 2.13 m	32.5
22	1.46 m	38.3	1.27 m	33.3	1.85 m	38.3
23	—	180.2	—	180.1	—	180.1
24	1.17 s	12.2	1.54 s	13.1	1.54 s	12.3
25	0.99 s	15.0	0.85	16.4	0.83 s	15.6
26	0.81	16.7	1.05	17.9	0.92 s	16.9
27	1.21 s	25.1	1.20	26.6	1.20 s	25.9
28	—	175.9	—	176.9	—	179.1
29	4.54 s	107.5	0.86	24.1	4.71 brs	106.9
30	—	—	0.87	33.6	—	—

Table 2 NMR data of sugar part of solysaponins B–D

	1		2		3	
Position	^{1}H	^{13}C	^{1}H	^{13}C	^{1}H	^{13}C
Glucose						
1	5.39 (d, J = 8.1 Hz)	95.6	6.29 (d, J = 8.3 Hz)	96.3		
2	3.11 (t, J = 8.3 Hz)	74.7	4.17 m	74.6		
3	3.26 m	78.5	4.00 (t, J = 9.4 Hz)	79.8		
4	3.30 m	70.9	4.32 (brd, J = 9.4 Hz)	71.6		
5	3.34 m	78.1	4.25 m	79.4		
6	3.61 m	62.3	4.44 (dd, J = 12.0, 2.6 Hz)	62.7		
	3.72 m		4.38 (dd, J = 12.0, 4.4 Hz)			
Glucuronic acid						
1	4.37 (d, J = 7.9 Hz)	105.5	5.19 (d, J = 7.9 Hz)	106.4	5.21 (d, J = 7.5 Hz)	105.7
2	3.72 m	76.3	4.06 (t, J = 8.5 Hz)	76.0	4.07 (t, J = 8.4 Hz)	75.1
3	3.28 m	77.1	4.20 m	78.3	4.21 (t, J = 8.8 Hz)	77.5
4	3.44 m	72.9	4.57 m	73.8	4.58 (t, J = 9.2 Hz)	73.1
5	3.35 m	78.1	4.60 m	78.4	4.62 m	77.6
6	—	171.2	—	173.2	—	172.4

connected to MPLC using a gradient elution of 0.1% formic acid (FA)/H_2O and 0.1% FA/ACN to get 18 fractions (Fr.1–1 to Fr.1–18). Subfraction Fr. 1–9 (102.0 mg) was purified over a recycling preparative HPLC and eluted with an isocratic mobile phase of H_2O-ACN-0.1% FA; 60 : 40 (flow rate: 6 mL min^{-1}) to get compound **1** (t_R = 10.5 min; 10.1 mg). Additionally, subfraction Fr. 1–10 (73.7 mg) was purified over a recycling preparative HPLC eluted with an isocratic mobile phase of H_2O-ACN-0.1% FA; 55 : 45 with flow rate: 5 mL min^{-1} to furnish compound **2** (t_R = 11.5 min; 12.6 mg). Moreover, subfractions Fr. 1–14 and Fr. 1–15 were purified over a recycling preparative HPLC eluted with H_2O-ACN-0.1% FA; 52 : 48 to get compounds **3** (t_R = 13.5 min; 20 mg) and **4** (t_R = 15.0 min; 8.2 mg). Subfraction Fr. 1–16 (85.0) mg was injected twice into a recycling preparative HPLC and eluted with a mobile phase of H_2O-ACN-0.1% FA; 52 : 48–40 : 60 to get compounds **5** (t_R = 23.5 min; 9.0 mg) and **6** (t_R = 25.0 min; 11.3 mg).

Solysaponin **B**; white amorphous powder; NMR (600 MHz, CD_3OD) see Tables 1, 2, Fig. 1 and 2; HRESIMS m/z 807.3809 [M–H]$^-$ (calculated for $C_{41}H_{59}O_{16}$, 807.3803).

Solysaponin **C**; white amorphous powder; NMR (600 MHz, C_5D_5N) see Tables 1, 2, Fig. 1 and 3; HRESIMS m/z 823.4123 [M–H]$^-$ (calculated for $C_{42}H_{63}O_{16}$, 823.4116).

Solysaponin **D**; white amorphous powder; NMR (600 MHz, C_5D_5N) see Tables 1 and 2. HRESIMS peak at m/z 645.3277 [M–H]$^-$ (calculated for $C_{35}H_{49}O_{11}$, 645.3275).

Antiviral assay

Viruses and cell line. The virus used in this study was the hCoV-19/Egypt/NRC-03/2020 SARS-CoV-2 isolate (GISAID

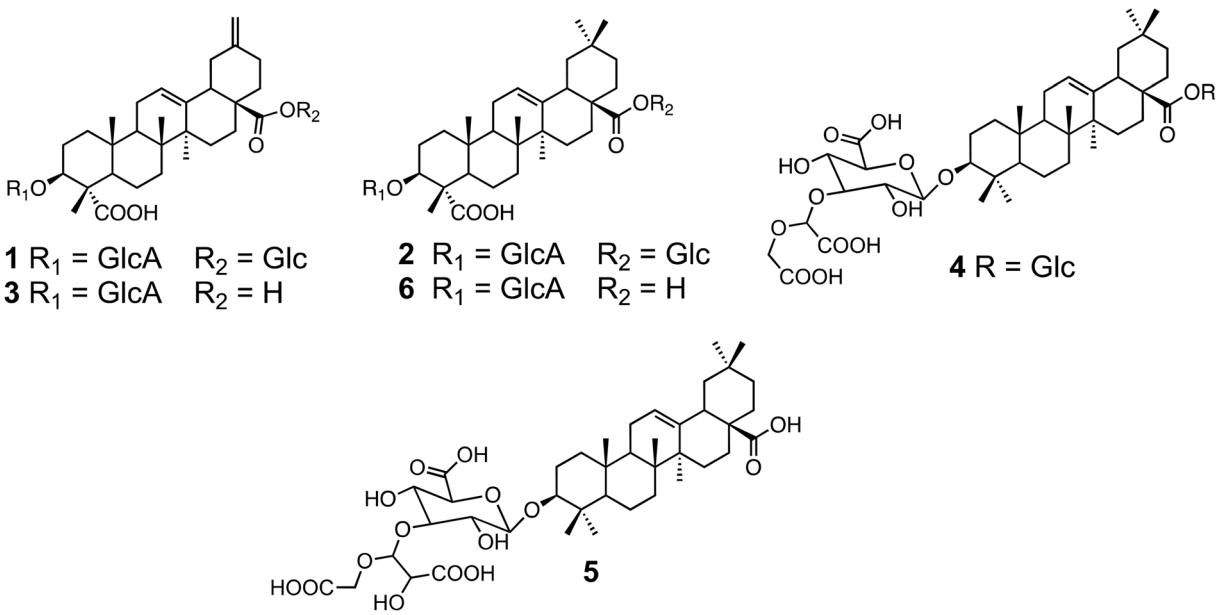

Fig. 1 Structure of the isolated compounds from *A. setifera* **1–6**.

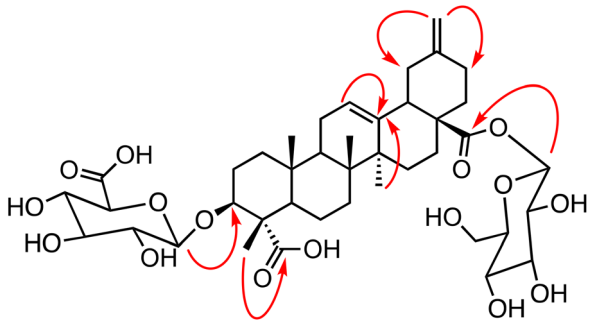

Fig. 2 HMBC correlations of solysaponin B.

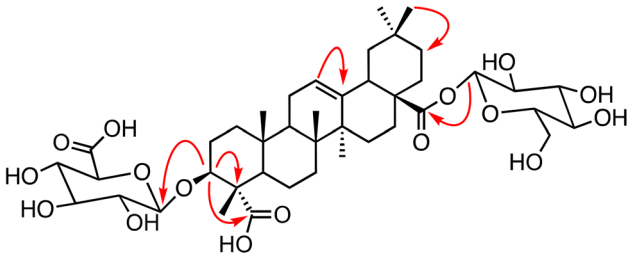

Fig. 3 HMBC correlations of solysaponin C.

Accession Number: EPI_ISL_430820). The African green monkey kidney (Vero E6) cells were kindly provided by Dr Richard Webby, St. Jude Children's Research Hospital, Department of Virology and Molecular Biology, USA. Vero-E6 cells were maintained in Dulbecco's Modified Eagle's Medium (DMEM) with 10% Fetal Bovine Serum (FBS) and 1% penicillin-streptomycin mixture at 37 °C and 5% CO_2. To propagate the virus, Vero E6 cells were infected with the virus at a multiplicity of infection (MOI) of 0.1 in infection medium (DMEM with 2% FBS, 1% penicillin/streptomycin, and 1% L-1-tosylamido-2-phenylethyl chloromethyl ketone (TPCK)-treated trypsin). Three days after infection, cell culture supernatant was collected and centrifuged for 5 min at 2500 rpm to eliminate cell debris. The supernatant was then aliquoted and titrated using Tissue Culture Infection Dose 50% ($TCID_{50}$) End-Point Dilution.

Determination of half maximal cytotoxic concentration (CC_{50}). To determine the 50% cytotoxic concentration (CC_{50}) of the tested compounds (**1–6**), stock solutions were prepared in Dulbecco's Modified Eagle Medium (DMEM) and serially diluted to get working concentrations ranging from 1 ng mL^{-1} to 1 mg mL^{-1}. The CC_{50} of each test compound was evaluated in Vero E6 cells using the crystal violet assay. Briefly, Vero E6 cell suspension (100 μL) was seeded into 96-well plates at a density of (3×10^5 cell per mL) and incubated at 37 °C in a humidified incubator with 5% CO_2 for 24 hours. Following incubation, the cell monolayers were treated with varying concentrations of each compound in triplicate. After 72 hours, the supernatants were discarded, and the monolayers were washed with phosphate-buffered saline (PBS). Cells were then fixed with 10% formaldehyde for 1 hour at room temperature. After drying, the monolayers were stained with 0.1% crystal violet for 20 minutes. The wells were subsequently washed, dried, and the crystal violet dye was dissolved using 200 μL methanol for 20 minutes on a bench rocker. Absorbance was measured at 570 nm using the Anthos Zenyth 200rt plate reader (Anthos Labtec Instruments, Heerhugowaard, Netherlands). Cytotoxicity at various concentrations was assessed relative to untreated controls, and CC_{50} values were determined *via* nonlinear regression analysis by plotting log inhibitor concentration against the normalized response.[13,14]

Determination of half inhibitory concentration (IC_{50}). The half-maximal inhibitory concentration (IC_{50}) values for compounds **1–6** was determined using a previously reported method.[13,14] Vero E6 monolayers, cultured in 96-well tissue culture plates, were washed once with phosphate-buffered saline (PBS). The hCoV-19/Egypt/NRC-3/2020 SARS-CoV-2 strain (NRC-03-nhCoV, $TCID_{50}$ = 100) was incubated with serial dilution and non-cytotoxic concentrations of the test compounds at 37 °C for 1 hour. The Vero-E6 cells were treated with virus and sample mixtures and kept at 37 °C for 1 h. Untreated, infected cells referred as the virus control, while untreated, uninfected cells referred as the cell control. Following 72 hours of incubation at 37 °C in a humidified 5% CO_2 incubator, the cell monolayers were fixed with 100 μL of 10% formaldehyde for 20 minutes and stained with 0.1% crystal violet (prepared in distilled water) for 15 minutes at room temperature. After staining, 100 μL of methanol was added to each well, and the optical density (OD) was measured at 570 nm using the Anthos Zenyth 200rt plate reader (Anthos Labtec Instruments, Heerhugowaard, Netherlands). The IC_{50} values were determined using nonlinear regression analysis by plotting the log inhibitor concentration against the normalized response. The selectivity index (SI) was calculated using the formula: $SI = CC_{50}/IC_{50}$.

Analysis of sugar units in the isolated solysaponins B–D (1–3). Each compound (2 mg) was mixed with 5% HCl (4 mL) at 95 °C for 4 h. The mixture was then extracted with CH_2Cl_2 (3×5 mL) and the aqueous layer was dried with methanol many times using a rotary vacuum evaporator. Then, the analysis by HPLC was conducted *via* an Agilent set of 1260 infinity II LC (Agilent Technologies, Santa Clara, CA, USA) with ELSD detector. Using Asahipak NH_2P-50 4E (4.6 × 250 mm), the authentic standards and the released sugars after hydrolysis were analyzed with an isocratic eluent system of H_2O–ACN (25 : 75). Finally, the sugar moieties were determined by comparison with authentic samples including D-glucuronic acid (5.5 min) and D-glucose (27.0 min).

Results and discussion

Identification of the isolated compounds

In this study, the aerial parts of *A. setifera* were extracted with 80% aqueous methanol to get the crude methanolic extract for chemical investigation. The crude extract was then partitioned through liquid–liquid fractionation, followed by a Diaion HP-20, reverse phase flash chromatography, and various rounds of HPLC purification to eventually afford six triterpenoid oleanane saponins (**1–6**). Among them, solysaponin **B–D** were

characterized as new ones. Additionally, among the isolated compounds from *A. asetifera* in this study, three known triterpene saponins **4–6** were identified as spinacoside C (achyranthoside E) (**4**),[15,16] betavulgaroside IV (**5**),[17] and (3β)-3-(β-D-glucuronopyranosyloxy)olean-12-en-23,28-dioic acid (**6**)[18,19] as shown in Fig. 1.

Solysaponin **B** (**1**) was obtained as a white amorphous powder, $[\alpha]_D^{25}$ −29.0 (*c* 0.02, C_5H_5N). Its structure was elucidated with the molecular formula of $C_{41}H_{60}O_{16}$ based on the HRESIMS peak at *m*/*z* 807.3809 $[M–H]^-$ (calculated for $C_{41}H_{59}O_{16}$, 807.3803). The HRESIMS showed an ion at *m*/*z* 645.3272 indicating the loss of a glucose moiety. The ^{1}H NMR spectrum of **1** (Table 1) revealed one hydroxymethine signal at δ_H 3.97 (H-3) correlated in HSQC with a carbon signal at δ_C 85.1. Additionally, the ^{1}H NMR spectrum indicated the presence of four tertiary methyl singlets at δ_H 0.91, 0.99, 1.17, and 1.21. The olefinic proton signal was determined at δ_H 5.24 and correlated in HSQC with a carbon signal at δ_C 123.9 as shown in Fig. 2. The olefinic carbon and the signal of a quaternary carbon at δ_C 144.1, indicated a Δ^{12} pentacyclic triterpene derivative. The 30-noroleanene type derivative was confirmed by the correlation of *exo*-methylene protons at δ_H 4.55 (δ_C 107.5) with two methylenes at δ_C 42.7 (C-19) and 30.8 (C-21) in the HMBC spectrum. Beside the signal of a glucuronic acid at δ_C 171.2, the APT NMR spectrum of **1** revealed two additional downfield shifted signals at δ_C 175.9 and 180.2 for C-28 and C-23 indicating two carboxyl groups in the aglycone part. In addition, two anomeric proton signals at δ_H 4.37 (J = 7.9 Hz) and 5.39 (J = 8.1 Hz) in the ^{1}H NMR spectrum revealing a β-orientation of the glycosidic linkage. Moreover, the cross-peaks of δ_H 4.37 with C-3 (δ_C 85.1) of the aglycone, and δ_H 5.39 with C-28 at δ_C 175.9 confirmed the attachment of two sugars at positions C-3 and C-28 of the aglycone. Finally, the structure of **1** was identified as 3-*O*-β-D-glucuronopyranosyl-3β-hydroxy-30-noroleane-12,20(29)-diene-23,28-dioic acid 28-*O*-β-D-glucopyranosyl ester and named as solysaponin **B**.

Solysaponin **C** (**2**) was obtained as a white powder, $[\alpha]_D^{25}$ −23.0 (*c* 0.02, C_5H_5N). Its structure was elucidated with the molecular formula of $C_{42}H_{64}O_{16}$ based on the HRESIMS peak at *m*/*z* 823.4123 [M–H]− (calculated for $C_{42}H_{63}O_{16}$, 823.4116). The ^{1}H NMR spectral data of solysaponin C (**2**) revealed six methyl groups resonated at δ_H 0.85 (3H, s, H-25), 0.86 (3H, s, H-29), 0.87 (3H, s, H-30), 1.05 (3H, s, H-26), 1.20 (3H, s, H-27); a characteristic olefinic proton at δ_H 5.38 (t, J = 3.6 Hz); an oxygen-bearing methine at 4.68 (dd, J = 12.0, 4.5 Hz), and two anomeric protons at δ_H 6.29 (d, J = 8.3 Hz) and 5.19 (d, J = 7.9 Hz). The APT and HSQC NMR data of **2** revealed 42 carbon signals, assigned for 6 methyls, 11 methylenes, 15 methines (one olefinic and two anomeric), and 10 quaternary carbons (including one olefin and three carbonyl) as shown in Table 1. Apparently, the two carbon signals resonated at δ_C 123.2 and 144.6 (C-12 and C-13) proposed a triterpene oleanane type. The existence of two sugar moieties were confirmed by signals at δ 5.19 (d, J = 7.9 Hz)/106.4 and 6.29 (d, J = 8.3 Hz)/96.3 as deduced from correlations in HSQC experiment. Additionally, the HMBC cross-peaks of anomeric protons at δ_H 5.19 with δ_C 85.7 (C-3) and δ_H 6.29/176.9 (C-28) indicated that two sugars, β-D-glucose, and β-D-glucuronic acid, were attached to C-28 and C-3, respectively. Further, the presence of sugars, β-D-glucose and β-D-glucuronic acid, were confirmed by the analysis with high-performance liquid chromatography (HPLC) after acid hydrolysis of compound **2** with 5% HCl and comparison with authentic sugar standards. Moreover, the location of a carboxylic group was proved to be C-23 by the correlation of H-3 at δ_H 4.68 (dd, J = 12.0, 4.5 Hz) with δ_C 180.1 (C-23) as obtained in HMBC spectrum. Finally, **2** was deduced to be 3-*O*-β-D-glucuronopyranosyl-28-*O*-β-D-glucopyranosyl-olean-12-en-3β-ol-28-oic acid, namely solysaponin **C** (**2**).

The structure of solysaponin **D** (**3**), $[\alpha]_D^{25}$ −24.0 (*c* 0.02, C_5H_5N), was determined with the molecular formula of $C_{35}H_{50}O_{11}$ based on the HRESIMS peak at *m*/*z* 645.3277 $[M–H]^-$ (calculated for $C_{35}H_{49}O_{11}$, 645.3275), which was the same as that of compound **1** except in absence of glucose moiety at C-28. On the basis of the comparison of the APT and ^{1}H NMR data as shown in Table 1, solysaponin **D** was supposed to be similar to that of **1** with the presence of a glucouronic acid attached to C-3 but differs in the absence of a glucose moiety from C-28. The ^{1}H and APT NMR data showed characteristic signals for the aglycone moiety; the presence of four singlet methyls [(δ_H 0.83/δ_C 15.6), (0.93/δ_C 16.9), (1.21/δ_C 25.9), (1.54/δ_C 12.4)], an olefinic proton at [δ_H 5.43 (t, J = 3.8 Hz)/δ_C 122.5], one oxymethine proton at δ_H 4.70/δ_C 85.9, one anomeric proton δ_H 5.21 (d, J = 7.5 Hz)/δ_C 105.6, and one *exo*-methylene protons at δ_H 4.71/δ_C 106.9. Moreover, the existence of three carboxyl groups was indicated by signals resonated at δ_C 180.1, 179.1, 172.4. The HMBC cross peaks (Fig. 3) further confirmed the structure of **3** that was established as 3-*O*-β-D-glucouronopyranosyl-3β-hydroxy-30-noroleane-12,20(29)-diene-23,28-dioic acid and named as solysaponin **D**.

Cytotoxicity and antiviral activity against SARS-CoV-2

The cytotoxic concentration (CC_{50}) of the isolated triterpene saponins was determined using a cytotoxicity assay, whereas the inhibitory concentration (IC_{50}) was assessed through an antiviral activity assay. The *in vitro* antiviral activity of saponins isolated from the halophyte *A. setifera* was evaluated, revealing pronounced inhibition activities against the tested virus. The therapeutic potential was determined through determination of half-maximal inhibitory (IC_{50}) and cytotoxic (CC_{50}) concentrations, with subsequent calculation of the selectivity index (SI) as a key measure of antiviral efficacy. The results of antiviral assay against SARS-CoV-2 revealed that the isolated triterpene oleanane saponins from the methanol extract of *A. setifera* exhibit promising anti-viral activity as illustrated in Table 3. Interestingly, compound **1** demonstrated a potent anti-viral activity with a cytotoxic concentration (CC_{50}) of 522 μg mL^{-1} and an inhibitory concentration (IC_{50}) of 2.339 μg mL^{-1}, resulting in selectivity index (SI) of 223.1 for SARS-CoV-2. The antiviral activity of **1** (IC_{50} = 2.339 μg mL^{-1}) against SARS-CoV-2 was stronger than remdesivir with an IC_{50} of 4.55 μg mL^{-1}, SI = 61.45. Additionally, compounds **2** and **4** exhibited potent antiviral activity with half-maximal inhibitory concentrations (IC_{50}) of 6.837 and 4.038 μg mL^{-1}, respectively. Their selectivity indices (SI) were 65.6 and

Table 3 Antiviral activity of isolated compounds from the halophyte *Anabasis setifera* against SARS-CoV-2

	Cytotoxic concentration (CC_{50})	Inhibitory concentration (IC_{50})	
A. setifera compounds	Vero-E6 (μg mL^{-1})	SARS-CoV-2 (μg mL^{-1})	Selectivity index (SI)
1	522.0	2.339	223.17
2	448.6	6.837	65.61
3	972.8	26.83	36.25
4	347.7	4.038	86.10
5	192.5	$IC_{50} < CC_{50}$	—
6	428.9	31.48	13.62
Remdesivir	279.6	4.55	61.45

86.10, respectively. Conversely, compounds **3** and **6** showed moderate activity with IC_{50} values of 26.83 and 31.48, respectively, and their selectivity indices (SI) were 36.25 and 13.62, respectively.

Concerning the tested oleanane-type triterpene saponins **1** to **6**, those comprising an additional glucose moiety at C-28, *i.e.*, **1**, **2** and **4**, demonstrated potent anti-SARS-CoV-2 activity, with IC_{50} values ranging between 2.339 and 6.837 μg mL^{-1}, whereas compounds **3** and **6**, lack this sugar moiety, are moderate active agents with IC_{50} values of 26.83 and 31.48 μg mL^{-1}. Apparently, the most pronounced anti-SARS-CoV-2 effect was observed for the oleanane-type triterpene saponin **1**, comprising an *exo*-olefin moiety, which showed an IC_{50} value of 2.339 μg mL^{-1}. These findings indicate that *A. setifera* represents a promising source of bioactive compounds with antiviral properties, warranting further investigation for pharmacological development.

Conclusions

This study highlights the significant antiviral potential of triterpenoid oleanane saponins isolated from the halophyte *Anabasis setifera* Moq. against SARS-CoV-2. Six saponins (**1–6**) were identified, with solysaponin **B–D** (**1–3**) being reported for the first time. Notably, compounds **1**, **2**, and **4** exhibited promising antiviral activity, with IC_{50} values ranging between 2.339 and 6.837 μg mL^{-1}, while compound **1** emerged as the most effective, displaying a high selectivity index (SI = 223.1). The presence of a glucose moiety at C-28 appears crucial for enhanced antiviral activity, as evidenced by the superior efficacy of **1**, **2**, and **4** compared to their counterparts lacking this structural feature. These findings underscore the therapeutic potential of *A. setifera* as a potential source of bioactive compounds, particularly in the development of novel antiviral agents against SARS-CoV-2. Further mechanistic and *in vivo* studies are needed to explore the clinical applicability of these saponins in combating COVID-19 and other viral infections.

Conflicts of interest

The authors declare no competing interests.

Data availability

Data will be available upon request from the corresponding authors. The data supporting this work (Fig. S1–S25) are included in Supplementary information. See DOI: https://doi.org/10.1039/d5ra03089g.

Acknowledgements

The authors are indebted to Prof. Ibrahim A. El-Garf, Department of Botany, Faculty of Science, Cairo University, Egypt, for the identification of plant.

References

1 G. S. Caleffi, A. S. Rosa, L. G. De Souza, J. L. S. Avelar, S. M. R. Nascimento, V. M. De Almeida, A. R. Tucci, V. N. Ferreira, A. J. M. Da Silva, O. A. Santos-Filho, M. D. Miranda and P. R. R. Costa, *J. Nat. Prod.*, 2023, **86**, 1536–1549, DOI: 10.1021/acs.jnatprod.3c00249.
2 COVID-19 cases | WHO COVID-19 dashboard, https://data.who.int/dashboards/covid19/cases?n=c, accessed 17 March 2025.
3 A. Othman, Y. Amen and K. Shimizu, *Fitoterapia*, 2021, **152**, 104907, DOI: 10.1016/j.fitote.2021.104907.
4 M. Bueno and M.-P. Cordovilla, *Front. Plant Sci.*, 2019, **10**, 439, DOI: 10.3389/fpls.2019.00439.
5 D. Yang, N. Han, Y. W. Wang, J. X. Zhai, Z. H. Liu, S. K. Li and J. Yin, *J. Org. Chem.*, 2021, **86**, 11220–11236, DOI: 10.1021/acs.joc.1c00812.
6 N. L. Nguyen, T. H. Vo, Y. C. Lin, C. C. Liaw, M. K. Lu, J. J. Cheng, M. C. Chen and Y. H. Kuo, *J. Nat. Prod.*, 2021, **84**, 259–267, DOI: 10.1021/acs.jnatprod.0c00919.
7 A. Mroczek, *Phytochem. Rev.*, 2015, 577–605, DOI: 10.1007/s11101-015-9394-4.
8 J. M. Augustin, V. Kuzina, S. B. Andersen and S. Bak, *Phytochemistry*, 2011, **72**, 435–457, DOI: 10.1016/j.phytochem.2011.01.015.
9 K. Grabowska, W. Buzdygan, A. Galanty, D. Wróbel-Biedrawa, D. Sobolewska and I. Podolak, *Phytochem. Rev.*, 2023, **22**, 1–50, DOI: 10.1007/s11101-023-09864-1.
10 S. Chaudhary, V. Thomas, L. Todaro, O. Legendre, S. Pecic and W. W. Harding, *Nat. Prod. Commun.*, 2008, **3**(11), 1747–1750, DOI: 10.1177/1934578X0800301101.
11 M. Ferreira, D. Pinto, Â. Cunha and H. Silva, *Appl. Sci.*, 2022, **12**(15), 7493, DOI: 10.3390/app12157493.
12 M. A. Saleh, *J. Agric. Food Chem.*, 1986, **34**, 192–194.

13 M. Y. Zakaria, A. Abo Elmaaty, R. El-Shesheny, R. Alnajjar, O. Kutkat, S. Ben Moussa, A. Y. A. Alzahrani, S. El-Zahaby and A. A. Al-Karmalawy, *RSC Adv.*, 2024, **14**(52), 38778–38795, DOI: **10.1039/d4ra07316a**.

14 E. Abdelsalam, A. M. Ibrahim, A. A. El-Rashedy, M. S. Abdel-Aziz, O. Kutkat and F. K. Abd EL-Hady, *Sci. Rep.*, 2025, **15**, 685, DOI: **10.1038/s41598-024-77854-0**.

15 K. Kuwada, S. Kawase, K. Nakata, N. Shinya, Y. Narukawa, H. Fuchino, N. Kawahara and F. Kiuchi, *J. Nat. Med.*, 2020, **74**, 135–141, DOI: **10.1007/s11418-019-01355-y**.

16 M. Yoshikawa, T. Murakami, K. Hirano, H. Matsuda, J. Yamahara, K. Ohtani, R. Kasai and K. Yamasaki, *Heterocycles*, 1998, **49**, 93–96.

17 M. Yoshikawa, T. Murakami, M. Kadoya, H. Matsuda, O. Muraoka, J. Yamahara and N. Murakami, *Chem. Pharm. Bull.*, 1996, **44**, 1212–1217.

18 X. L. Chen, K. Zhang, X. Zhao, H. L. Wang, M. Han, R. Li, Z. N. Zhang and Y. M. Zhang, *Int. J. Mol. Sci.*, 2023, **24**(3), 2454, DOI: **10.3390/ijms24032454**.

19 C. Borel, M. P. Gupta and K. Hostettmann, *Phytochemistry*, 1987, **26**, 2685–2689, DOI: **10.1016/S0031-9422(00)83572-4**.